Technical Report

TR-07-08

Creep testing and creep loading experiments on friction stir welds in copper at 75°C

Henrik C M Andersson, Facredin Seitisleam, Rolf Sandström
Corrosion & Metals Research Institute

August 2007

Svensk Kärnbränslehantering AB
Swedish Nuclear Fuel
and Waste Management Co
Box 5864
SE-102 40 Stockholm Sweden
Tel 08-459 84 00
+46 8 459 84 00
Fax 08-661 57 19
+46 8 661 57 19

Creep testing and creep loading experiments on friction stir welds in copper at 75°C

Henrik C M Andersson, Facredin Seitisleam, Rolf Sandström
Corrosion & Metals Research Institute

August 2007

Keywords: Creep, Creep loading, Copper, Nucklear waste disposal, Creep rate.

Abstract

Specimens cut from friction stir welds in copper canisters for nuclear waste have been used for creep experiments at 75°C. The specimens were taken from a cross-weld position as well as heat affected zone and weld metal. The parent metal specimens exhibited longer creep lives than the weld specimens by a factor of three in time. They in turn were longer than those for the cross-weld and HAZ specimens by an order of magnitude. The creep exponent was in the interval 50 to 69 implying that the material was well inside the power-law breakdown regime. The ductility properties expressed as reduction in area were not significantly different and all the rupture specimens demonstrated values exceeding 80%. Experiments were also carried out on the loading procedure of a creep test. Similar parent metal specimens and test conditions were used and the results show that the loading method has a large influence on the strain response of the specimen.

Background

Nuclear waste from fuel elements will be highly radioactive for thousands of years. During this time it must be kept away form living organisms. The current plan in Sweden for long term disposal is to place the waste in containers deep in the bedrock. The containers will be surrounded with bentonite clay. The containers are designed to stay intact for more than 100,000 years /1/.

The containers themselves consist of a load bearing insert made of nodular cast iron. This is then placed in an outer shell made of extruded copper /2/. The purpose of the copper canister is to act as corrosion barrier. Lids have to be welded to the shell, even though the bottom lid might be manufactured integral with the shell by using the pierce and draw method. The thickness of the copper shell is 50 mm. To allow for placement of the iron insert in the copper shell, a gap of about 2 mm must be present between the iron and the copper. This gap will close after placement in the repository due to external hydrostatic pressure as the bentonite clay is saturated by groundwater. This process is calculated to continue for approximately one hundred years. The temperature of the container during this time is estimated to about 80–90°C. This temperature is high enough to allow for the deformation of the copper by creep. If the creep ductility is high enough the deformation can occur without any cracks forming. The maximum strain in the copper is about 5% /1/. Including a safety factor a uniaxial creep ductility of at least 10% is needed to avoid cracking. The copper and the welds must exhibit at least this creep ductility in testing. The temperature will decrease to the level of the surrounding bedrock, 15°C, during the first thousand years of the containment /1/.

Studies of the creep properties of copper alloys intended for nuclear waste disposal has been undertaken since the late 1980's. At first oxygen free copper was tested in the interval 75 to 350°C /3, 4, 5, 6, 7/ but the latest studies have progressively moved towards the lower temperature end of this interval more like those expected in the repository. To obtain sufficient creep ductility the oxygen free copper has to be doped with about 50 ppm phosphorous /8, 9, 10/. Work has also been performed on the recrystallisation and extrusion properties of the same chemical composition copper /11, 12/.

The greatest strain concentrations in the copper shell are located at the interface between the lid and the shell, where the weld is located. The ductility properties of the weld is thus of great interest. The technical difficulties in thick-walled copper welding are significant. Several different weld methods have been considered including electron beam welding. The choice now of weld method is friction stir welding /13/.

Previous creep testing of weld specimens has been performed on welds made in copper that had been roll-formed /9, 10/ and not extruded. Since the decision for the Swedish nuclear waste canisters is to use extrusion as the manufacturing method the aim of the work presented in this paper is to perform similar experiments on welds made from extruded material. Experience in the laboratory has also shown that the loading procedure affects the creep response of the copper, and a series of experiments was conducted to evaluate the effect.

Contents

1 Friction stir welding (FSW) in copper

Friction stir welding is a solid state (non-melting) welding process and has been shown to give welds with low density of defects and few discontinuities in the microstructure /14/. The mechanical properties are such that it is difficult to distinguish between parent metal, cross-weld and weld metal creep test experiments if only the test results are studied /9, 10/.

The weld is made by a tool that is rotating at a high rate and moving through the metal being joined, Figure 1-1. The tool itself is ribbed to improve the stirring of the metal around the tool, Figure 1-3. The metal is not melted but rather just "swirled" around the tool. In this way the metal is thoroughly mixed at a relatively high temperature. Measurements indicate that the highest macroscopic temperature is around 800°C /15/. This temperature is high enough to recrystallise the material during cooling of the weld. Most stresses from the welding should therefore be relaxed during the cooling down process. A thorough description of the FSW method and a modelling study of the welding process can be found in /16/.

Important parameters in the FSW process are the rotational speed of the tool, the pressure by which the tool is pressed down into the component and the translational speed of the tool. The tool is composed of a central pin mounted in the centre of a flat plate called the shoulder that rotates along with the pin. The shoulder pressing on the work piece generates most of the frictional heat, not the rotating pin. This can be seen in a cross-section of a weld where the weld zone has a tulip like shape at the bottom of the weld but flaring towards the top surface, Figure 1-2. This is the case because the heat input of the shoulder and also because the shoulder moves part of the metal around with it. The resulting track of the shoulder can be seen in Figure 1-4.

The most common feature in the weld has been found to be the so called nugget that can be found in the middle of the weld in the wake behind the tool. /17/.

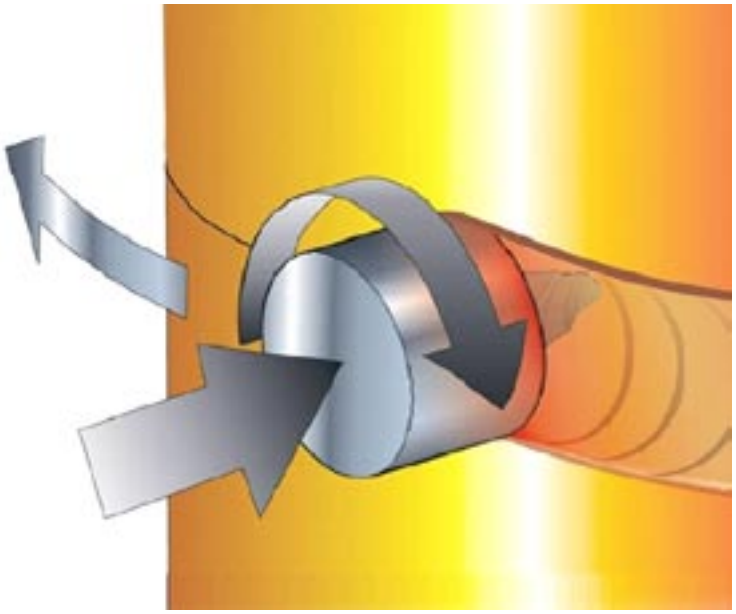

Figure 1-1. *Schematic drawing of the friction stir weld process.*

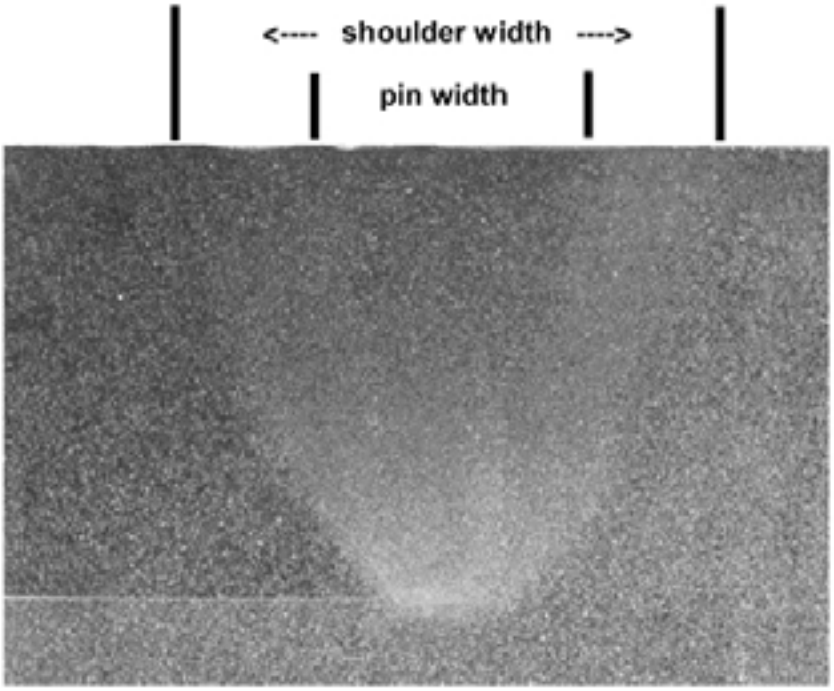

Figure 1-2. *Cross section of a typical FSW weld. In the bottom left part is the gap between the welded pieces of copper still visible. Note the flaring of the weld zone at the top of the weld where the shoulder has pressed at the material. The pin width at the base is marked in the image. The pin then tapers down to 25% width at the tip.*

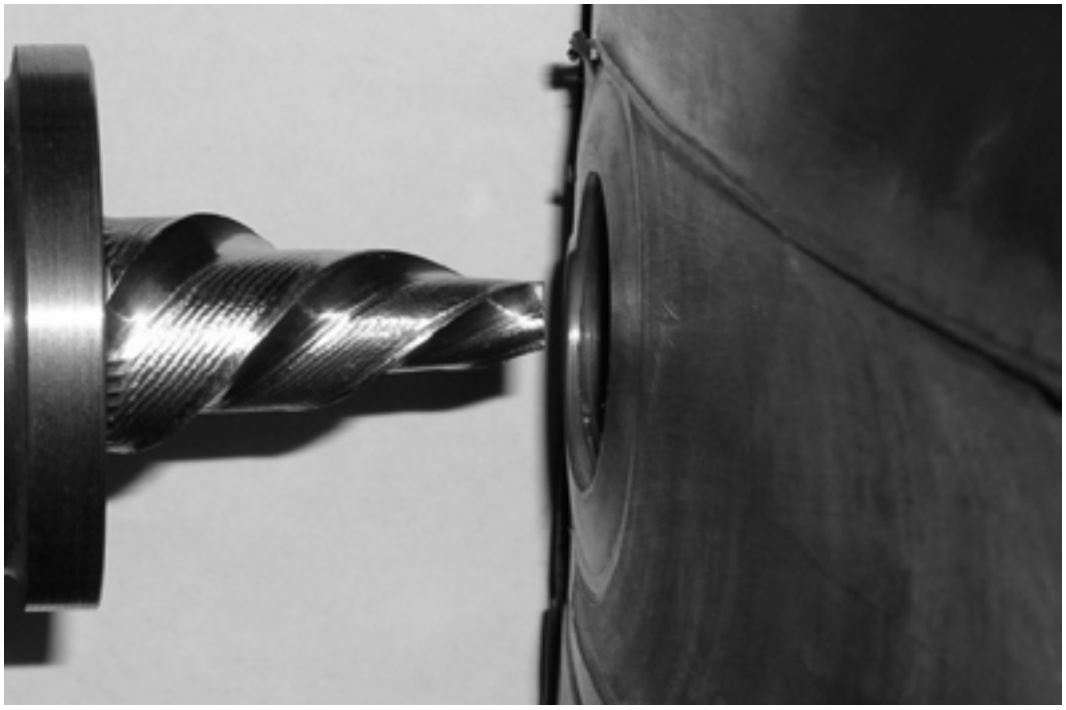

Figure 1-3. *FSW welding about to start. To the left of the image the tool is visible.*

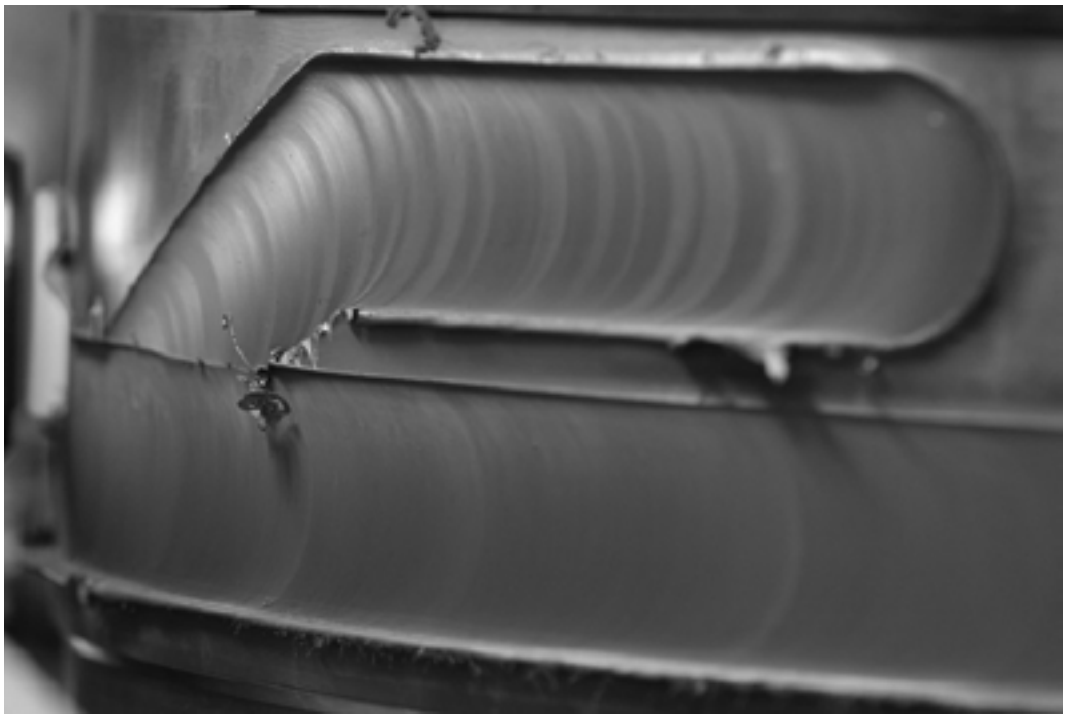

Figure 1-4. *The weld after fabrication. On the top of the weld is the start area where the tool is inserted and the weld begun. After the initial transients have abated the tool is lowered to the make the weld. When the whole weld is completed a certain overlap is made which is visible in the image, and then the tool is parked above the weld in a similar fashion as the start area. When the tool is finally withdrawn a hole results and this has to be placed in an area where it can be machined away.*

2 Experimental

The friction stir weld tested in this work was manufactured at the canister laboratory operated by the Swedish Nuclear Fuel and Waste Management Co (SKB). The weld had before being delivered to the creep lab been checked for weld defects and no significant defects had been found. An image of a cross section of the weld is shown in Figure 2-1. The nugget structure could not be observed in this weld.

From the weld creep test specimens were cut in cross-weld position and along the weld in weld metal position, see Figure 2-2. Specimens were also cut from the portion of the weld that could be deemed to be the heat affected zone. This is a structure that is difficult to observe in FSW welds but for this study the area directly beneath the shoulder tip was assumed to be the heat affected zone. In light optical microscopy this area shows up as the transition from fully recrystallised copper to tempered base metal. Base metal specimens were taken from both the forged lid and from the extruded tube.

Care was taken during the manufacture of the specimens to minimise the introduction of cold working, but no anneal was applied to the material either before or after the manufacturing step.

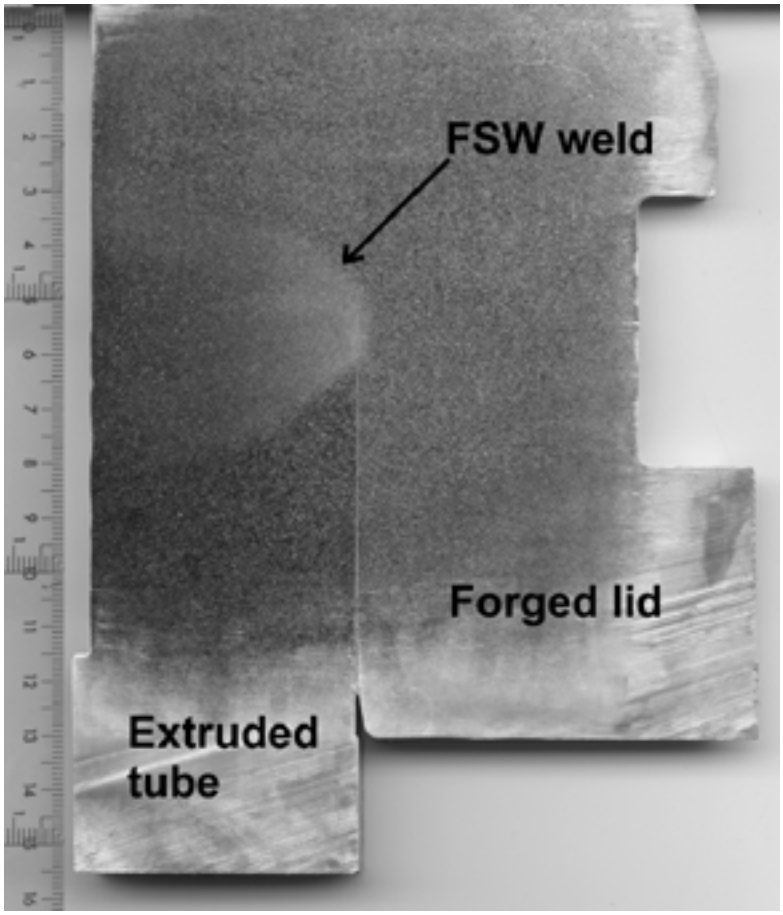

Figure 2-1. *Cross section of the friction stir weld. At the bottom a section of the extruded shell is seen and to the right the forged lid. The protruding lip at the top right corner is a circular lifting tab for handling of the manufactured canisters.*

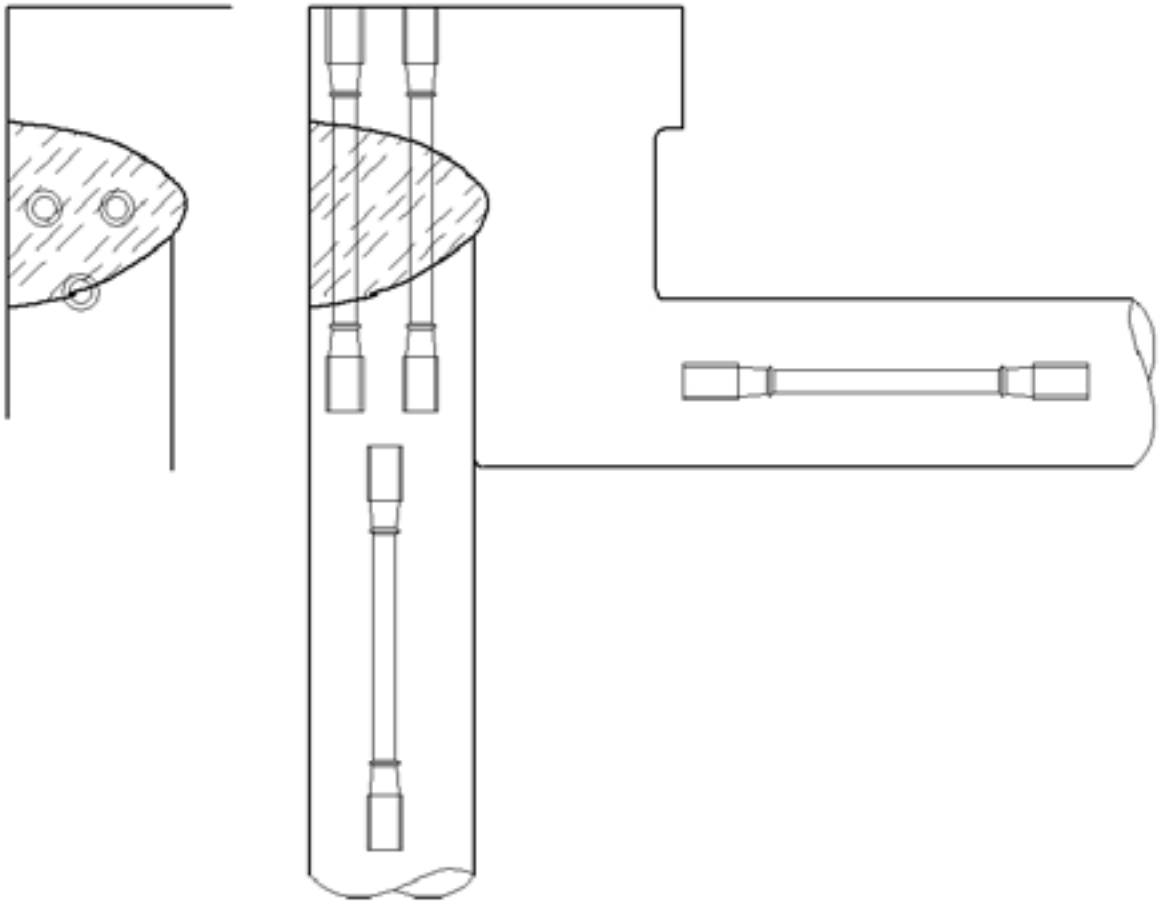

Figure 2-2. *Specimen extraction positions in cross-weld, weld metal and heat affected zone positions. Parent metal specimens were cut both from the shell and the lid as indicated.*

3 Results

3.1 Creep loading experiments

When the test is started the specimen is placed inside the furnace and heated to test temperature without any applied load. After the test temperature has been reached the specimen is allowed to soak for a few hours to guarantee that the specimen has reached a stable temperature and then the load is applied. The standard procedure is to apply the load stepwise and within 3 minutes from the start of the loading. During this initial loading the strain is measured and logged.

The loading strain in copper has previously been found to be large, sometimes as high as 15% /8, 9, 10/. Metals with an fcc crystal structure such as austenitic stainless steels often exhibit large initial strains, but usually at a lower magnitude. To study the effect of loading time several specimens were started with the same temperature and stress but with different loading rates. The loading times used were 3 minutes, 16, 166 and 483 hours. The results can be found in Figure 3-1 and Figure 3-2. As can be observed from the graphs the longer loading times give increased initial strain with the exception of the shortest loading which gives the highest initial strain. The reason for these differences is not readily apparent.

In Figure 3-3 the rest of the creep test after loading is shown for the same specimens. Two of the specimens have ruptured, one has been interrupted and one is still in testing. There is no apparent relationship between loading time and rupture time in the graph, but the analysis is complicated by the repeated reloads of the test rig. The maximum travel of the lever arm is about 5 mm at the specimen, which translates to about 5% strain. When this is reached the specimen has to be temporarily unloaded, the lever arm raised and finally the specimen is reloaded. Evidently this procedure yields a new primary stage each time, see Figure 3-3. Depending on the number of resets the strain develops differently for each test even though they are at the same nominal stress. Further investigations into the loading strain phenomena have to be performed without reloads. The test rigs are being modified to include this option.

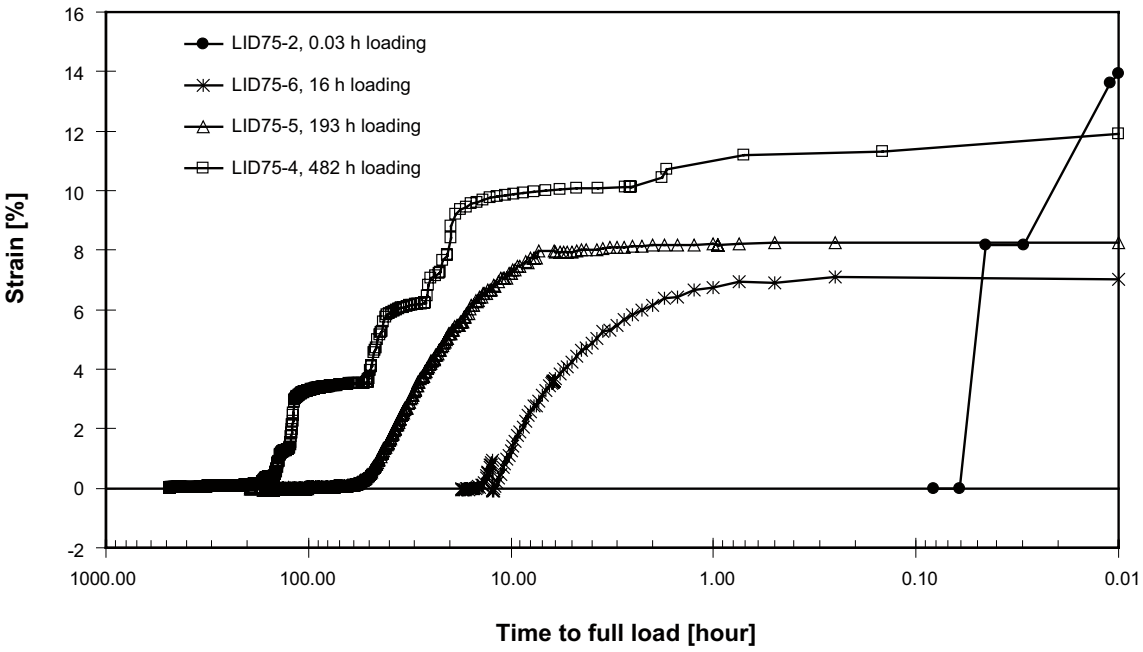

Figure 3-1. *Strain versus loading time for four specimens tested at 170 MPa, 75°C.*

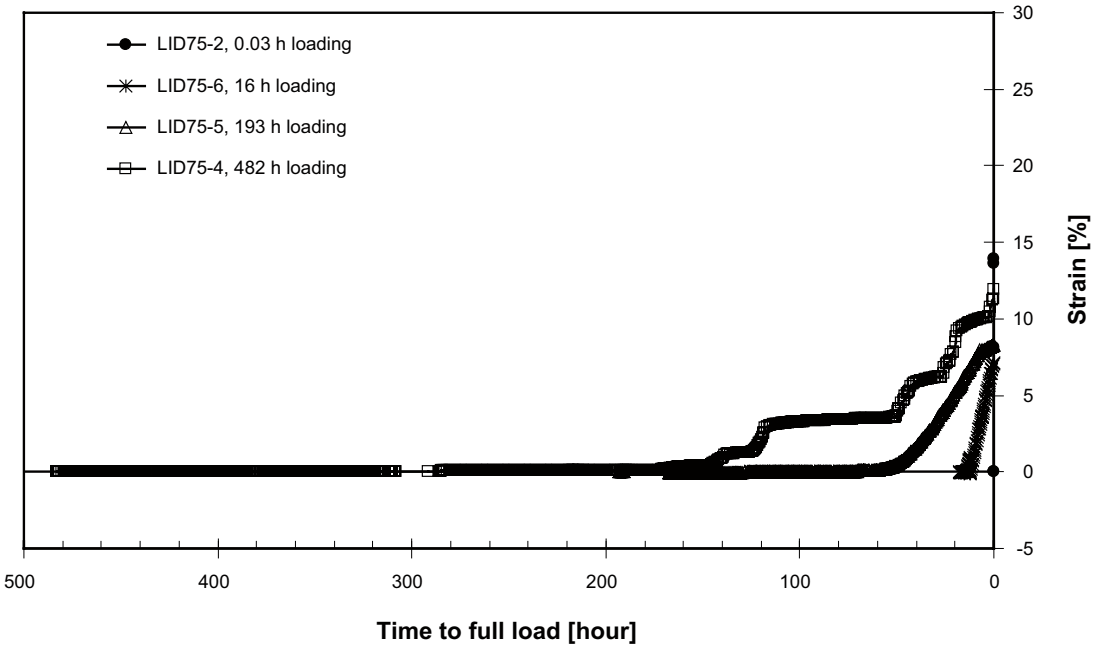

Figure 3-2. *Same as Figure 3-1 but with linear time on the x-axis.*

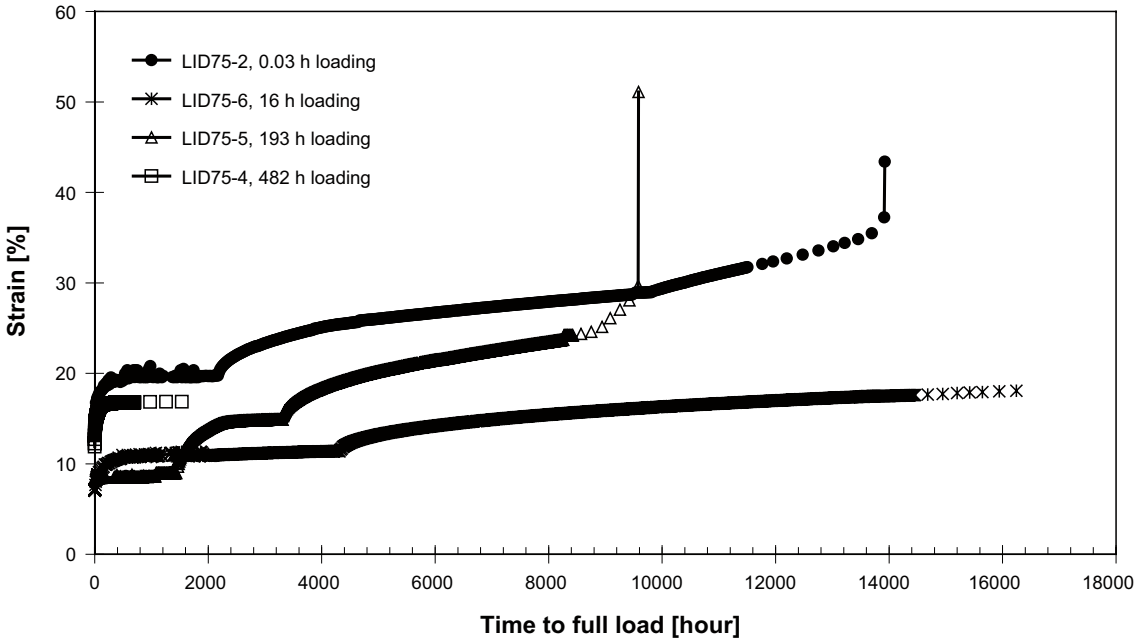

Figure 3-3. *The resulting creep curves after the loading described in Figure 3-1 and Figure 3-2. Note that specimen LID75-4 was interrupted after 1,500 h.*

3.2 Creep test results

The results from the creep rupture testing are given in Figure 3-4 where comparable specimens from an earlier investigation also have been included /10/. From the graph it can be observed that the two different tested base metals have the longest creep lives. Cross-weld specimens exhibit the shortest creep lives with the weld metal specimens in between. The heat affected zone specimens show similar creep lives as the cross-weld specimens, hinting that the creep

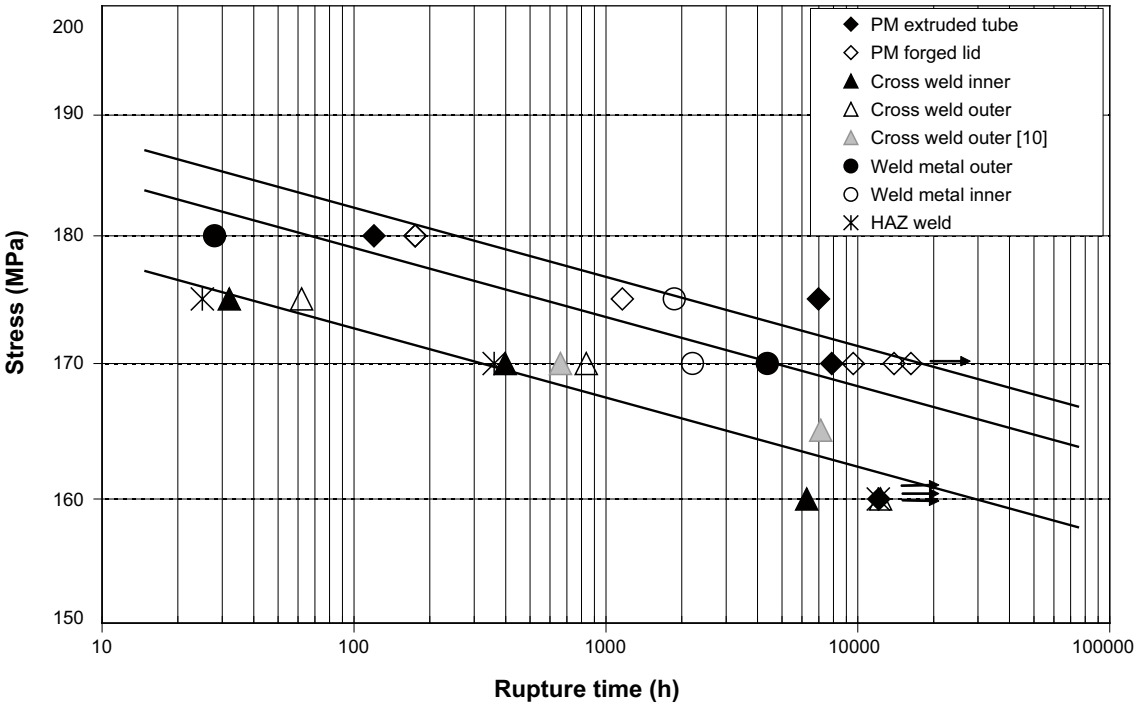

Figure 3-4. *Creep rupture time versus stress for all specimens. Arrows denote tests still running. Lines included in the graph are trendlines for the tests. From top to bottom parent metal, weld metal and cross-weld/HAZ. Data from /10/ are included for comparison.*

life of a cross weld specimen might be limited by the heat affected zone. Cross-weld specimens from the previous investigation have similar creep lives as cross-weld specimens from the present work.

The creep elongation is given in Figure 3-5 and the area reduction in Figure 3-6. Compared to the previous investigation the rupture strains in this investigation are generally higher, above 40%, and the area reduction comparable with values above 80%.

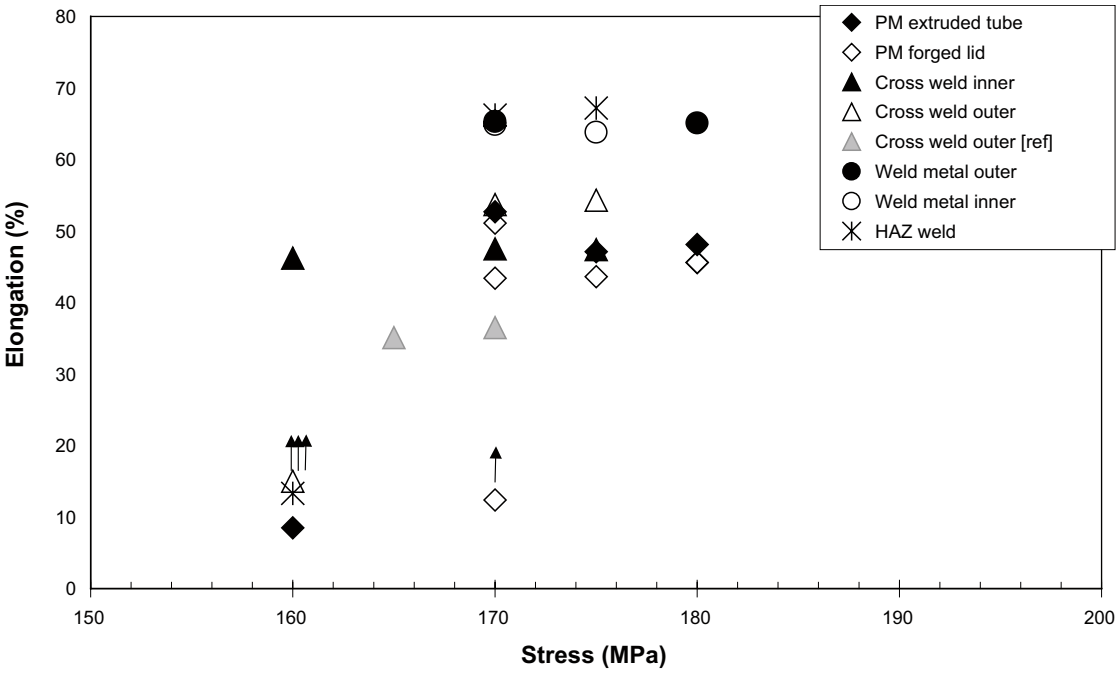

Figure 3-5. *Creep elongation versus stress for all specimens.*

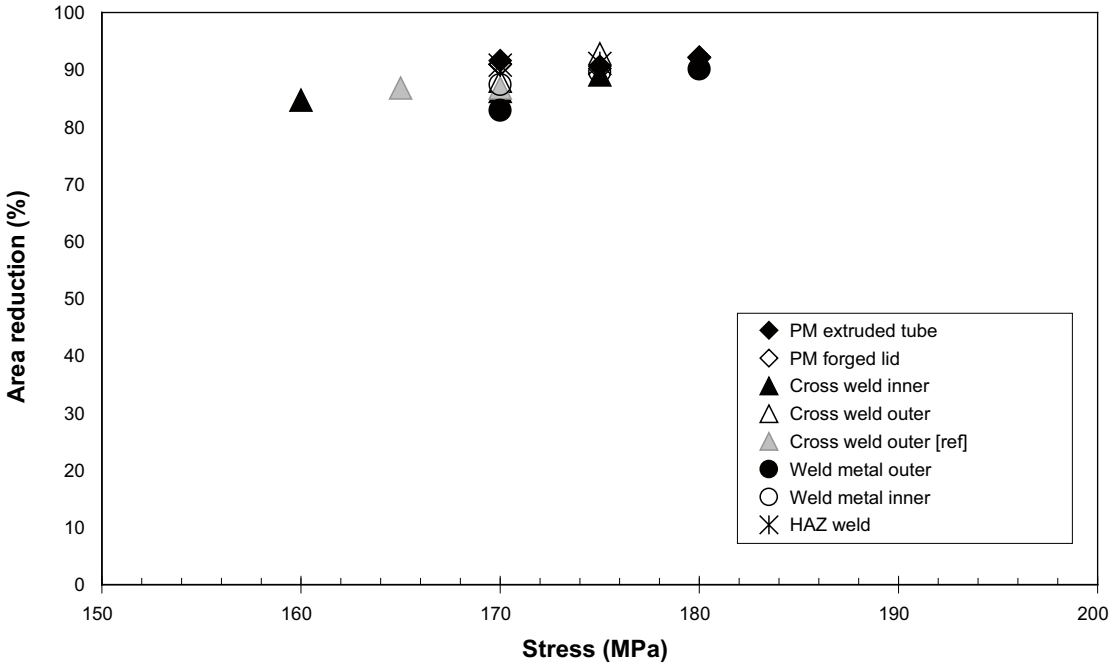

Figure 3-6. *Creep reduction of area versus stress for all ruptured specimens.*

In Figure 3-7 to Figure 3-10 the minimum creep rate versus stress for the friction stir welds is shown for parent metal, weld metal and cross-weld specimens respectively. The Norton exponent, *n*, in the power law creep equation (Equation 1) was found to be high.

$$\dot{\varepsilon} = A\sigma^n \qquad \text{(Equation 1)}$$

$\dot{\varepsilon}$ is the minimum creep rate, σ is the applied stress and A and n are constants. For the parent metal tests the Norton exponent was found to be 50, which corresponds to those measured previously. The exponent for the weld metal tests was 69, and the cross-weld tests showed a Norton exponent of 54.

As found from Figures 3-7 to Figure 3-10 the difference in creep exponent between the different microstructures is not very large and it is doubtful whether it is significant. For that reason a common exponent is proposed for modelling. The following relations are chosen

$$\dot{\varepsilon}_{PM} = 8 \cdot 10^{-130}\sigma^{54} \qquad \text{(Equation 2)}$$

$$\dot{\varepsilon}_{WM} = 40 \cdot 10^{-130}\sigma^{54} \qquad \text{(Equation 3)}$$

$$\dot{\varepsilon}_{HAZ} = 160 \cdot 10^{-130}\sigma^{54} \qquad \text{(Equation 4)}$$

$$\dot{\varepsilon}_{CW} = 400 \cdot 10^{-130}\sigma^{54} \qquad \text{(Equation 5)}$$

The creep rates for the parent metal (PM), weld metal (WM), heat affected zone (HAZ) and cross-welds (CW) are given. Equations 2 to 5 are illustrated in Figure 3-11. An adequate representation of data is obtained.

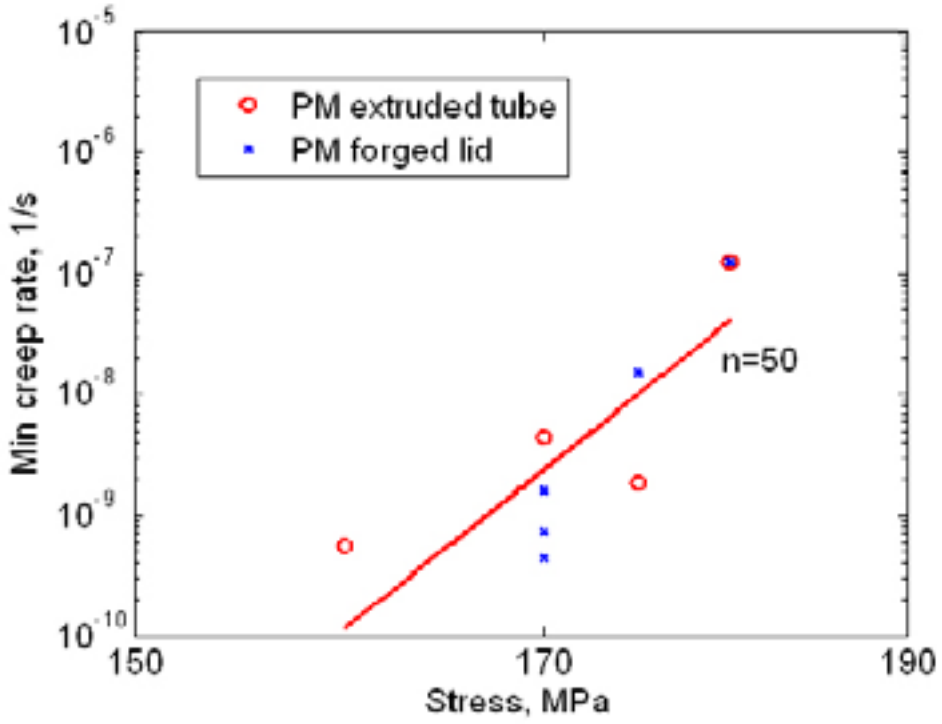

Figure 3-7. *Norton plot for parent metal specimens.*

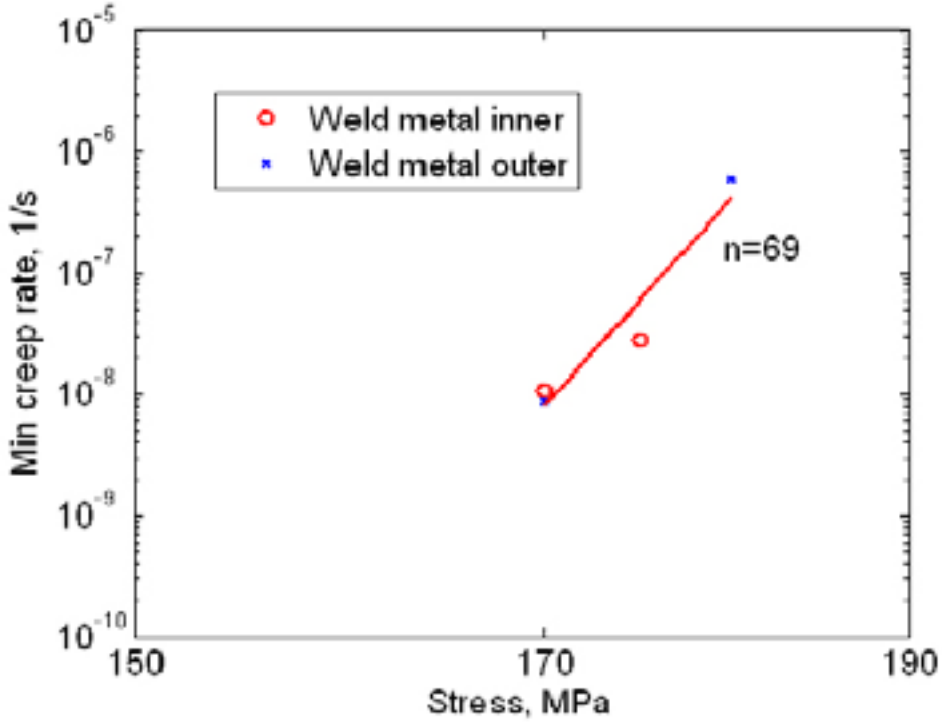

Figure 3-8. *Norton plot for the weld metal specimens.*

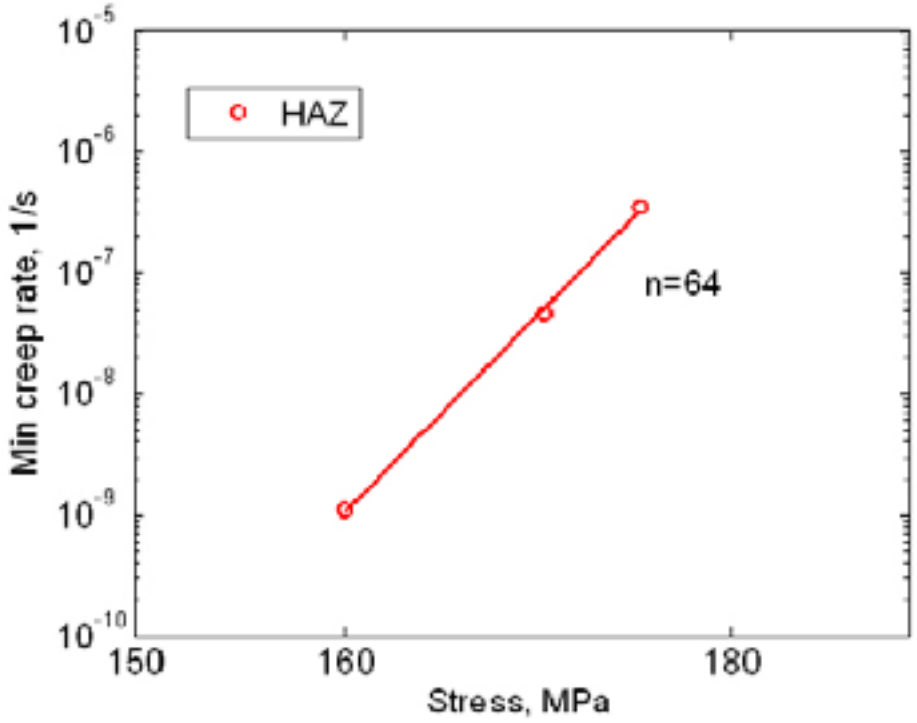

Figure 3-9. *Norton plot for the heat affected zone (HAZ) specimens.*

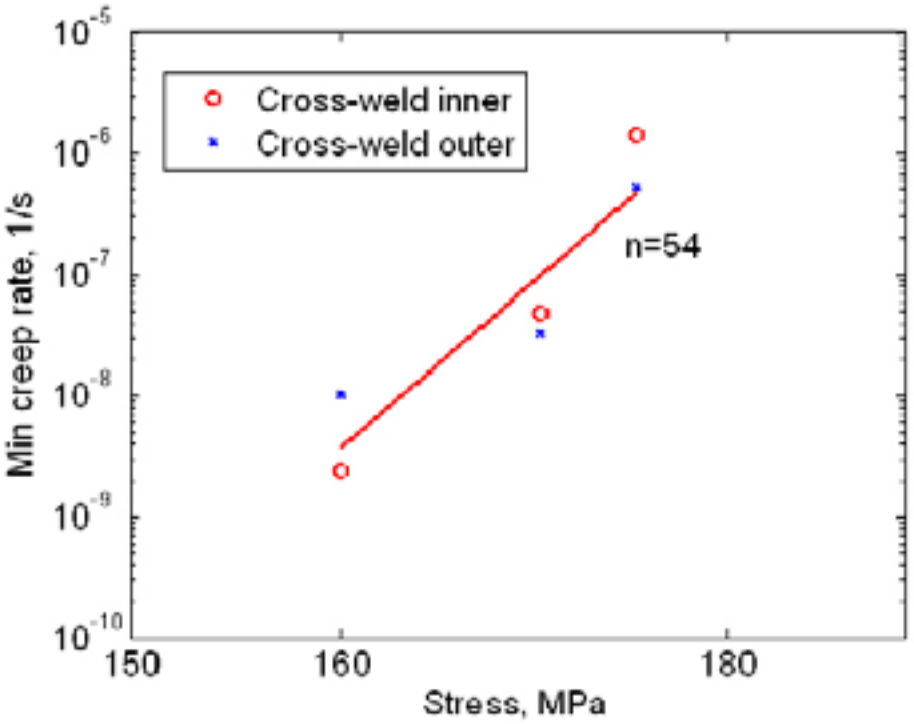

Figure 3-10. *Norton plot for the cross-weld specimens.*

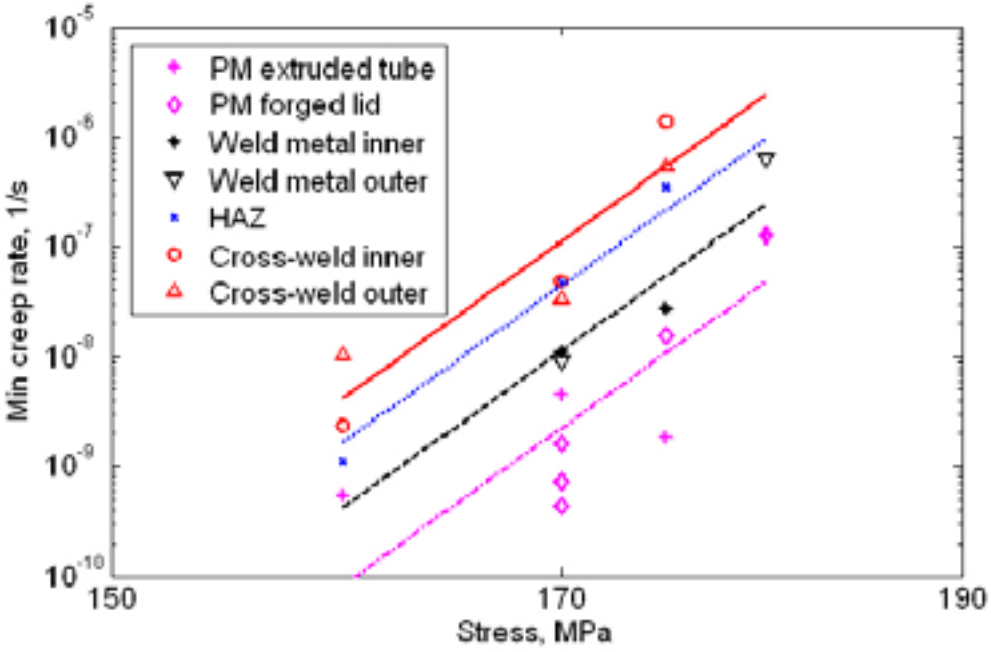

Figure 3-11. *Norton plot for all tested specimens (n = 54).*

3.3 Metallography

After testing selected specimens were prepared for metallography. The surface was etched to display the grains and the twin boundaries and the grain size estimated by comparison to standard micrographs. In Figure 3-12 to Figure 3-15 images of the unstrained material taken in a light optical microscope (LOM) are collected. The morphology was similar with equiaxed grains and visible twinning but the grain size varies. In the forged lid material, the grain size was 70 µm and in the extruded tube 100 µm. Twins could be observed in both materials but to a higher degree in the tube. The grain size of the weld metal was estimated to be around 200 µm and in the heat affected zone closer to 400 µm taken at a point roughly halfway through the thickness. The grain size varies with the depth and is usually smaller at the bottom of the weld, but this was not studied in this work.

The microstructure near the rupture in the weld metal specimens was distinguished by deformed and elongated grains and also some cavity formation, Figure 3-16. The same could be observed in the heat affected zone specimens. The formation of the cavities may be connected to the larger grain size in the weld. Previous investigations also showed similar cavities when large grain material was tested /8/. The cavities might be present also in the other specimens but due to the smaller grain size they could be obscured.

The cross weld specimens show that necking has started at two places within the gauge length, Figure 3-17. This corresponds to the heat affected zone parts of the gauge, and show that the HAZ is the creep weakest part of the weld.

Measurements of the hardness taken across the weld before testing are shown in Figure 3-18. The hardness does not vary significantly across the weld but stays between 70–80 HV0.05. After testing all weld parts have a hardness between 100 and 110 when measured far away form the necking. The reason for the increase could be the creep strain that the copper has experienced, somewhat akin to cold deformation.

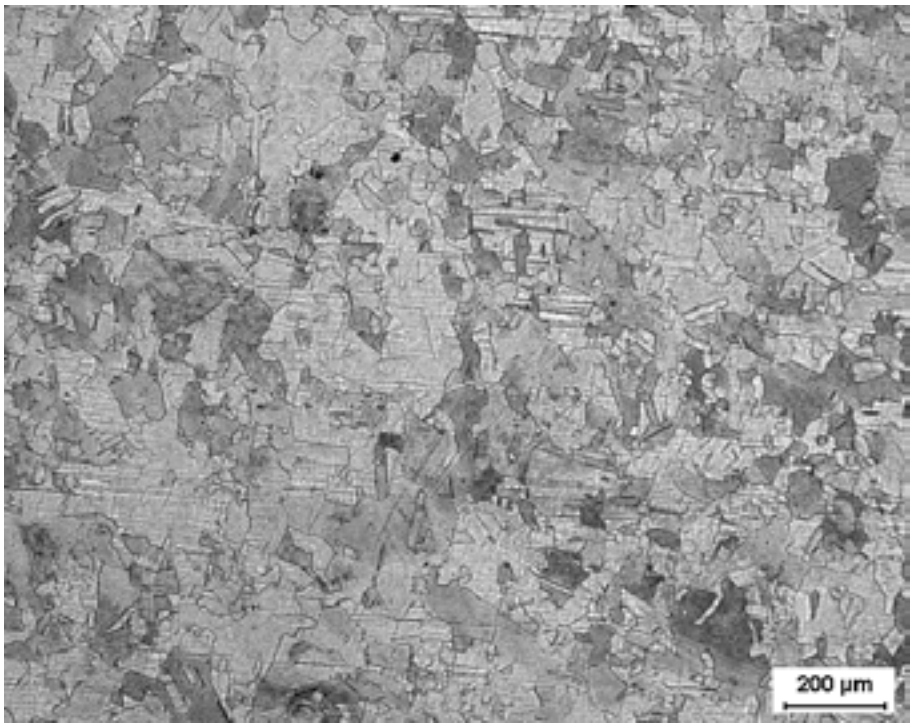

Figure 3-12. *Micrograph of the grain structure in the forged lid. Unstrained material. LOM 50x.*

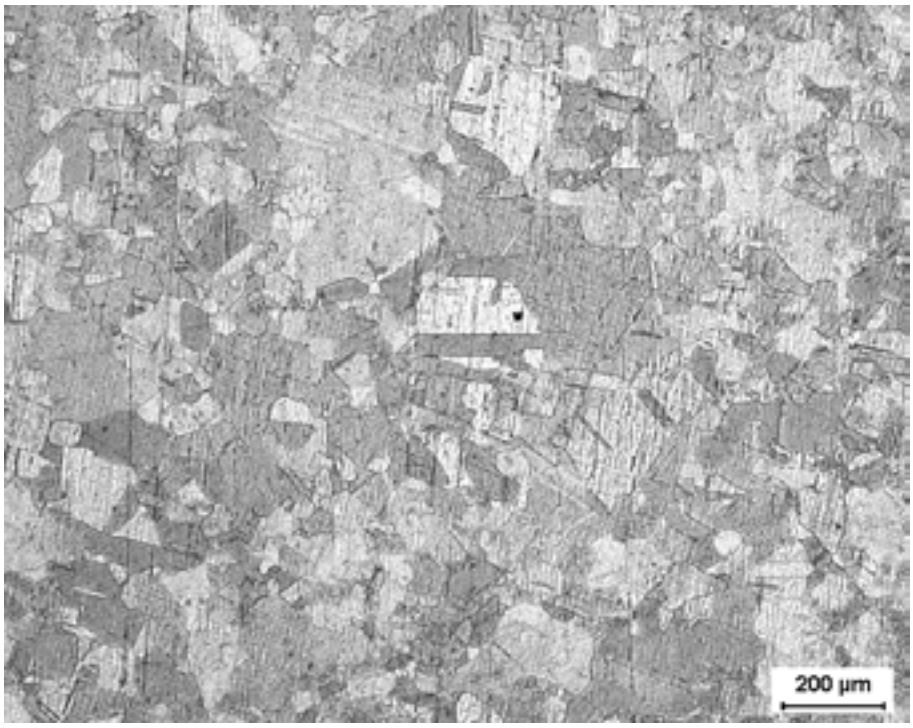

Figure 3-13. *Micrograph of the grain structure in the extruded tube. Unstrained material. LOM 50x.*

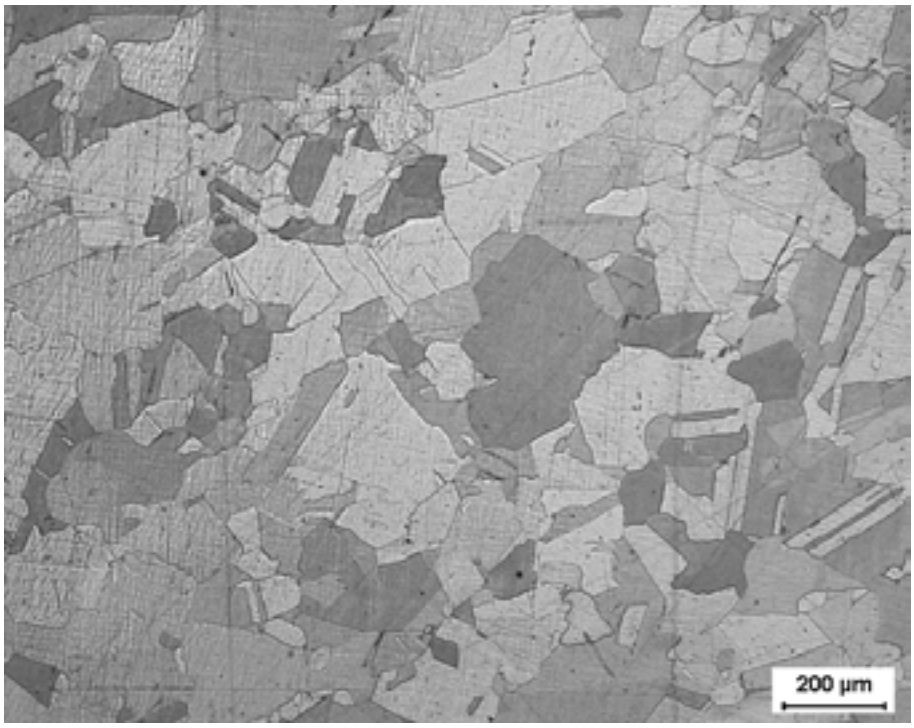

Figure 3-14. *Micrograph of the grain structure in the weld metal. Unstrained material. LOM 50x.*

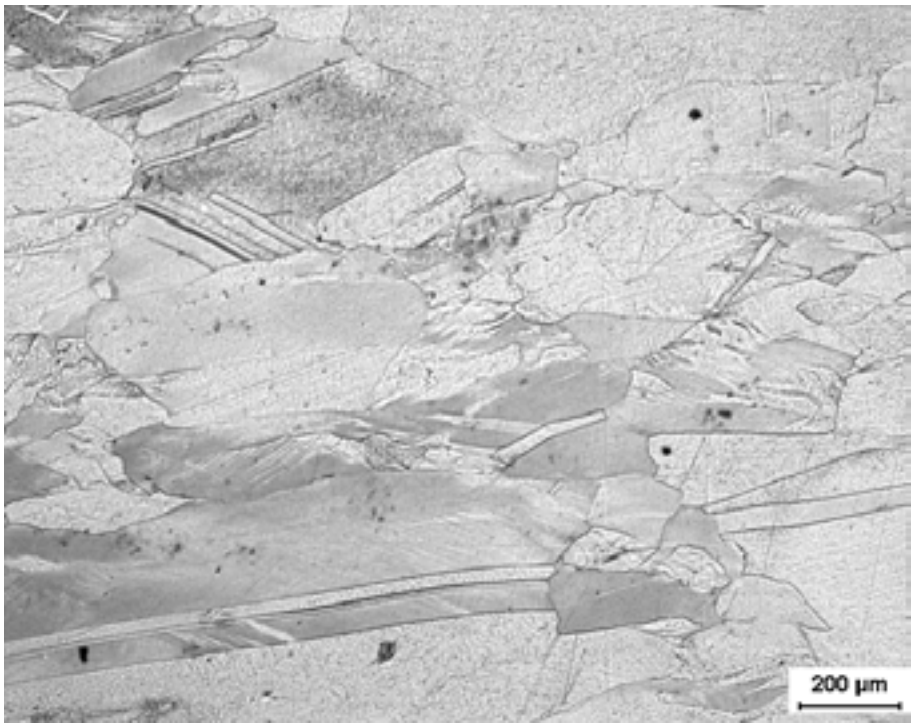

Figure 3-15. *Micrograph of the grain structure in the heat affected zone. Slightly strained material. LOM 50x.*

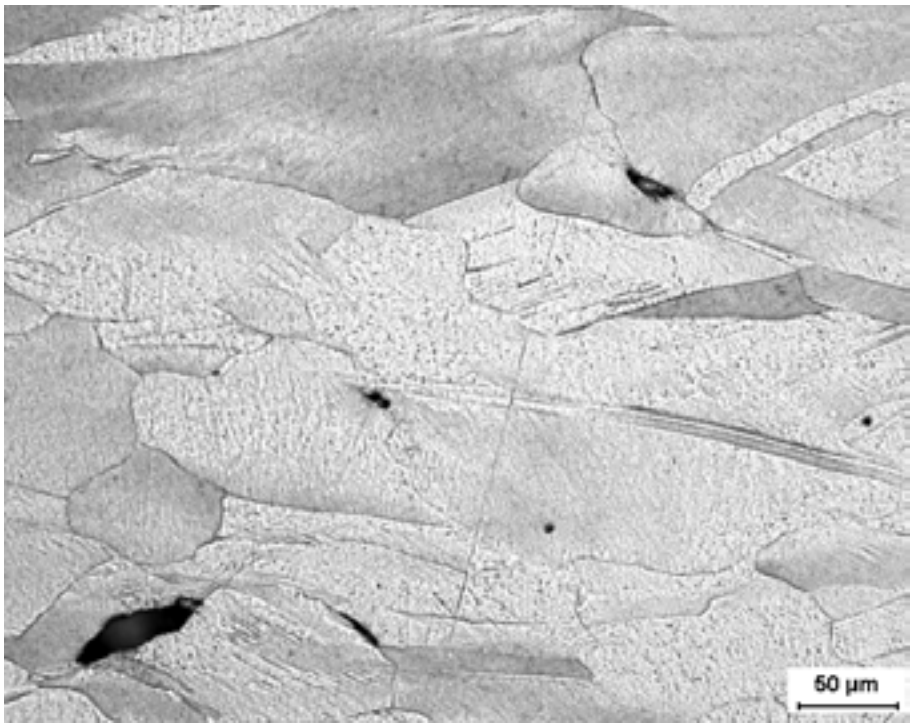

Figure 3-16. *Micrograph of the structure in a weld metal specimen 6 mm from the fracture. Cavities have formed at grain boundaries. LOM 200x.*

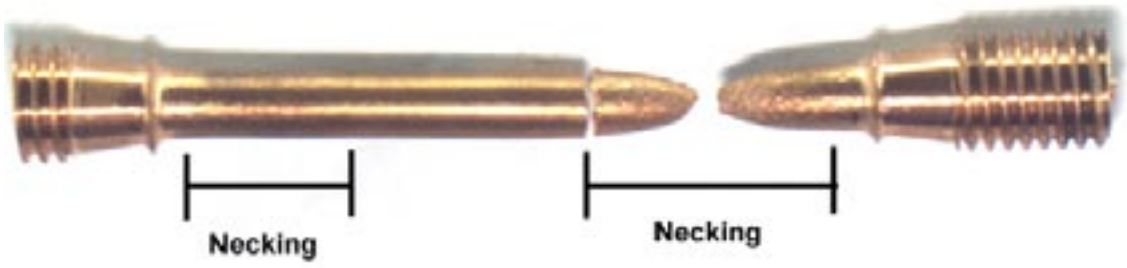

Figure 3-17. *A cross weld specimen after testing. Note the two necking areas, corresponding to the heat affected zone portions of the weld.*

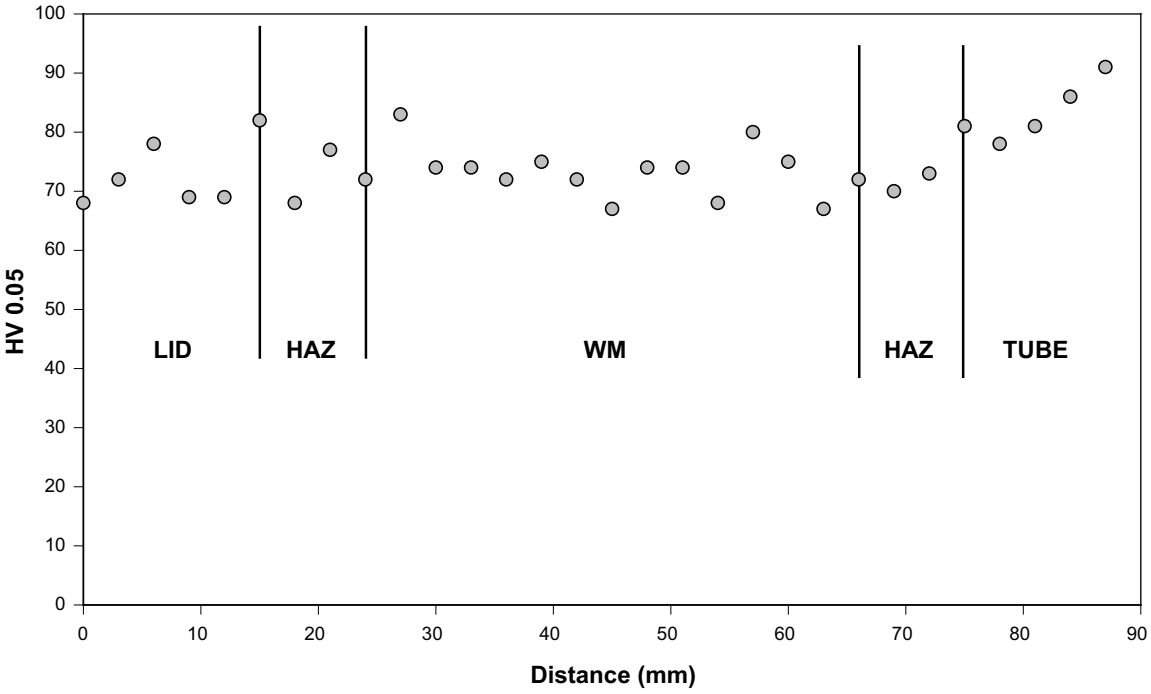

Figure 3-18. *Hardness across the weld prior to creep testing.*

4 Discussion and conclusions

The purpose behind the testing performed in this work has been to evaluate the creep properties at 75°C of a copper friction stir weld. The weld was performed by joining an extruded copper tube to a forged copper lid piece. Creep specimens taken from either of the two base materials showed the longest creep life. Creep specimens taken from within the weld metal had shorter creep lives, and cross-weld and heat affected zone specimens the shortest. The creep lives of the weld constituents are, even though this is not an aim of the test programme, generally longer than previously measured /9, 10/. No sharp inhomogenities is present in the welds and this is shown by the small difference in creep lives of the different weld parts.

Previous investigations have focussed on creep at higher temperatures than this work. The work presented in this study shows that the good ductility of phosphorous alloyed oxygen free copper is also present at 75°C. The creep ductility did generally exceed 40% and the area reduction 80%. This ductility is as high or higher than has previously been measured /3, 4, 8, 9, 10/. None of the tested specimens exhibited brittle creep rupture tendencies.

The microstructures in the weld and the parent metal are similar but with a difference in grain size. Both the forged tube and the extruded tube have smaller grain size than the weld metal. The largest grain size can be measured in the heat affected zone between the parent metal and the weld. This zone has also proven to be the weakest in creep both for the specimens taken wholly form within the heat affected zone and for the cross weld specimens. The heat affected zone is not softer than the other portions of the weld. This does not mean that the heat affected zone is softer than the rest of the weld. Hardness measurements have shown similar values across the weld.

The Norton creep exponent was measured to between 50 and 69, which is a high number. If the exponent is greater than 3–5 the material is said to be in the power-law breakdown area. Previous investigation has shown that Cu-OFP is well within this area at temperatures below 300°C /9, 10/. Recent papers have successfully linked the creep response in phosphorous alloyed copper to the solute drag effect on dislocation movement by the phosphorous atoms /18/. This effect has also been modelled /19/.

The way in which the load is applied is also important to the creep result and even more so to the initial strain. Several different loading times were applied to specimens tested under the same stress/temperature conditions. The loading strain varied from 6% to 14%. There was no clear correlation between loading time and initial strain, but this might be connected to the number of reloads a specimen is subjected to during the loading and also to the number of load increments. In further studies the load increments must be kept to an absolute minimum, and the loading time increased to months, rather than days.

The overall conclusion from the testing is that the creep properties at 75°C of the different parts of the weld are comparable with no part of the weld significantly weaker than the others. The maximum difference in strength between the different zones is 10 MPa. Creep ductility is high and adequate for the use in nuclear waste disposal copper canisters.

5 Acknowledgments

The authors wish to thank Svensk Kärnbränslehantering AB (Swedish Nuclear Fuel and Waste Management Company, SKB) for funding this work and supplying the test material.

References

/1/ **Werme L, 1988.** Design premises for canister for spent nuclear fuel, SKB TR-98-08, Svensk Kärnbränslehantering AB.

/2/ **Andersson C-G, 1998.** Test manufacturing of copper canisters with cast inserts Assessment report. SKB TR-98-09, Svensk Kärnbränslehantering AB.

/3/ **Henderson P J, Sandström R, 1998.** Low Temperature Creep Ductility of OFHC Copper, Materials science and engineering A, Vol. 246, no. 1–2, pp. 143–150.

/4/ **Seitisleam F, Henderson P J, Lindblom J, 1996.** Creep of copper for nuclear waste containment – Results of creep and tensile tests on Cu-OF, Cu-OFP, cathode copper and welded joints. Swedish Institute for Metals Research, Report IM–3327, Stockholm, Sweden.

/5/ **Henderson P J, 1994.** Creep of Copper, International Seminar on Design and Manufacture of Copper Canisters for Nuclear Waste, Sollentuna, Sweden, April 1994.

/6/ **Henderson P J, Werme L, 1996.** Creep testing of copper for radwaste canisters, Materials and Nuclear Power, EUROMAT 96, Bournemouth, United Kingdom, October 1996.

/7/ **Sandström R, 1999.** Extrapolation of creep strain data for pure copper, Journal of Testing and Evaluation, JTEVA, Vol. 27, No. 1, pp. 31–35.

/8/ **Andersson H C M, Seitisleam F, Sandström R, 1999.** Influence of phosphorous and sulphur as well as grain size on creep in pure copper, SKB TR-99-39, Svensk Kärnbränslehantering AB.

/9/ **Andersson H C M, Seitisleam F, Sandström R, 1999.** Creep testing of thick-wall copper electron beam and friction stir welds at 75, 125 and 175°C. SKB TR-05-08, Svensk Kärnbränslehantering AB.

/10/ **Andersson H C M, Seitisleam F, Sandström R, 2004.** Creep testing of thick-wall copper electron beam and friction stir welds, (abridged version of /9/) MRS Spring Meeting, San Francisco, 12–16 April, Mat. Res. Soc. Symp. Proc. Vol. 824, pp 51–56.

/11/ **Siwecki T, Petterson S, Blaz L, 1999.** Modelling of microstructure evolution and flow stress behaviour in association with hot working of Cu-P alloys, Swedish Institute for Metals Research, Report IM-1999-513, Stockholm, Sweden.

/12/ **Hamzah S, Stålberg U, 2001.** Grain size as influenced by process parameters in copper extrusion, Scandinavian Journal of Metallurgy. Vol. 30, no. 4, pp. 232–237.

/13/ **SKB, 2006.** Kapsel för använt kärnbränsle – Svetsning vid tillverkning och förslutning SKB R-06-04, Svensk Kärnbränslehantering AB.

/14/ **Källgren T, Sandström R, 2003.** 4th International Symposium on FSW, 14–16 May, Park City, USA, ISBN 1-903761-01-8, Session 3B. Paper S03B-P2.

/15/ **Källgren T, Jin L-Z, Sandström R, 2004.** Finite Element Modelling of Friction Stir Welding on Copper Canister, 5th International Friction Stir Welding symposium, Metz, France, 14–16, September.

/16/ **Källgren T, 2005.** Friction Stir Welding of Copper Canisters for Nuclear Waste, ISBN 91-7283-974-0, ISRN KTH/MSE--05/02-SE+MAT/AVH, Department of Materials Science and Engineering, Royal Institute of Technology (KTH), S-100 44 Stockholm, Sweden.

/17/ **SKB, 2006.** Reliability in sealing of canister for spent nuclear fuel. SKB R-06-26, Svensk Kärnbränslehantering AB.

/18/ **Sandström R, Andersson H C M, 2007.** The effect of phosphorus on creep in copper, J. Nucl. Mater.

/19/ **Sandström R, Andersson H C M, 2007.** Creep during power law breakdown in phosphorous alloyed copper, Proceedings of CREEP8 8th Int. Conf. on Creep and Fatigue at Elevated Temperatures, July 22–26, 2007, San Antonio, Texas.

ISSN 1404-0344
CM Digitaltryck AB, Bromma, 2007